A Versatile Platform to Incorporate Viral Trimeric Antigens into Self-Assembling Nanoparticle Immunogens

Baoshan Zhang[1*], Cara W. Chao[1*], Yaroslav Tsybovsky[2], Adam S. Olia[1], Guillaume Stewart-Jones[1], Raffaello Verardi[1], Shuishu Wang[1], Tongqing Zhou[1], and Peter D. Kwong[1¶]

[1] Vaccine Research Center, National Institute of Allergy and Infectious Diseases, National Institutes of Health, Bethesda, Maryland, United States of America

[2] Electron Microscopy Laboratory, Cancer Research Technology Program, Leidos Biomedical Research Inc., Frederick National Laboratory for Cancer Research, Frederick, MD 21701, USA.

[*] These authors contributed equally to this work.

¶ Corresponding author (PDK) Email: pdkwong@nih.gov

Abstract

Antigens displayed on self-assembling nanoparticles can stimulate strong immune responses and have been playing an increasingly prominent role in structure-based vaccines. However, the development of such immunogens may be complicated by inefficiencies in their production, especially with the metastable glycosylated trimeric type 1 fusion machines that are prevalent viral vaccine targets. To alleviate this issue, we developed a plug-and-play platform using the spontaneous isopeptide-bond formation of the SpyTag:SpyCatcher system to display trimeric antigens on self-assembling nanoparticles, including the 60-subunit *Aquifex aeolicus* lumazine synthase (LuS) and the 24-subunit *Helicobacter pylori* ferritin. LuS and ferritin coupled to SpyTag expressed well in a mammalian expression system when an *N*-linked glycan was added to the nanoparticle surface. Respiratory syncytial virus fusion (F) glycoprotein trimer – stabilized in the prefusion conformation by multiple disulfides and fused with SpyCatcher – could be efficiently conjugated to LuS-SpyTag or to ferritin-SpyTag, enabling multivalent display of F trimers with prefusion antigenicity. Similarly, F-glycoprotein trimers from human parainfluenza virus-type 3 and spike-glycoprotein trimers from SARS-CoV-2 could be displayed on LuS nanoparticles with decent yield and antigenicity. The versatile platform described here thus allows for multivalent plug-and-play presentation on self-assembling nanoparticles of trimeric antigens from viral respiratory pathogens, including the recently identified SARS-CoV-2.

Introduction

Self-assembling nanoparticles are playing an increasingly prevalent role in vaccine development as vaccine vehicles and immunomodulators. The appeal of nanoparticle immunogens lies in their inherent multivalent display of antigens, which is known to elicit robust B cell responses (reviewed in [1]). There have been numerous efforts to genetically fuse viral immunogens to nanoparticles within prokaryotic and eukaryotic systems, utilizing direct genetic fusion of antigenic molecules with self-assembling nanoparticle monomers [2-4], chemical conjugation [5,6], and a spontaneous intramolecular isopeptide bond formation with the SpyTag:SpyCatcher system [7,8], and some of these nanoparticles are now entering clinical trials [2,9,10].

Another important factor to consider in viral immunogen design is glycosylation. Viral pathogens are often heavily glycosylated, often as a means to evade the human immune system. Moreover, many viral antigens require glycosylation to be stably expressed and correctly folded. Although several studies have described plug-and-play nanoparticle systems [11-16], many use prokaryotic expression systems, which are not suitable to produce glycosylated antigens. Furthermore, *N*-glycans can be manipulated in immunogen design to selectively cover up unwanted epitopes as well as to improve the solubility and stability of immunogens [17-19]. Another factor to consider is that metastable type 1 fusion machines are prevalent vaccine targets [20].

Here we develop a modular self-assembling nanoparticle platform that allows for the plug-and-play display of trimeric viral glycoproteins on nanoparticle surfaces, utilizing the SpyTag:SpyCatcher system. We tested this system with three prefusion (preF)-stabilized viral trimeric glycoproteins: respiratory syncytial virus fusion (RSV F) glycoprotein [21], human parainfluenza virus type 3 fusion glycoprotein (PIV3 F) [22], and SARS-CoV-2 spike (S) glycoprotein [23,24]. SpyTag-coupled nanoparticles could express with sufficient yield from a mammalian expression system after the addition of nanoparticle surface glycans. Moreover,

protein antigens and nanoparticle scaffolds could be produced independently before conjugation, thereby expediting the otherwise generally cumbersome process of making and troubleshooting immunogens genetically fused to self-assembling nanoparticle subunits. Such a modular nanoparticle assembly platform may thus be a useful tool for plug-and-play screening of trimeric viral immunogens in a multivalent highly immunogenic context.

Results

Expression of LuS- and ferritin-nanoparticle scaffolds with SpyTag requires the addition of an *N*-linked glycan

To construct a reliable plug-and-play platform for nanoparticle presentation of antigens, we chose *Aquifex aeolicus* lumazine synthase (LuS) [25] and *Helicobacter pylori* ferritin [26] as nanoparticle scaffolds with SpyTag:SpyCatcher conjugation system [15] to display antigens on nanoparticle surface. The SpyTag:SpyCatcher system is highly specific and stable with an isopeptide bond and has been used for conjugation of antigens on nanoparticle surfaces [7,27] (Fig. 1a). LuS and ferritin have served as scaffolds for nanoparticle immunogens in a number of clinical studies: for LuS see https://www.clinicaltrials.gov/ct2/show/NCT03699241 [28]; for ferritin, see https://www.clinicaltrials.gov/ct2/show/NCT03547245 [10,29,30]. The N terminus of both ferritin and LuS are exposed to the nanoparticle surface and are thus accessible for SpyTag or SpyCatcher attachment (Fig. 1b). The C terminus of LuS is also assessible on the nanoparticle surface and can be used to display purification tags. We designed mammalian expression constructs expressing fusion proteins of SpyTag or SpyCatcher with LuS or ferritin. The constructs included both His- and Strep-tags for purification purposes, along with a signal peptide for secretion of the expressed proteins to the medium (Fig. 1b).

Initial constructs yielded low levels of expression for the nanoparticle-SpyTag or SpyCatcher fusion proteins. To improve protein solubility and expression, we added glycans to the surface of the nanoparticles, designing a panel of LuS and ferritin constructs with SpyTag and SpyCatcher (Table 1). For LuS constructs, we added a glycosylation site at position 71 (PDB 1HQK numbering). For ferritin constructs, two potential glycosylation sites (96 and 148) were tested. Addition of *N*-linked glycosylation sites facilitated expression of the nanoparticles. Three of the constructs produced decent yields of well-assembled nanoparticles, LuS with N71 and SpyTag at N-terminus (hereafter referred to as LuS-N71-SpyTag), ferritin with N96 and SpyTag, and ferritin S148 (glycan at N146) and SpyTag (Table 1). Of the two ferritin constructs, the ferritin with N96 and SpyTag had a higher yield and was chosen for further studies (hereafter referred to as ferritin-N96-SpyTag). Size exclusion chromatography (SEC) and electron microscopy (EM) analyses indicated that LuS-N71-SpyTag formed a homogeneous nanoparticle population in solution (Fig. 1c,d). The ferritin-N96-SpyTag sample comprised mainly of intact nanoparticles with some minor unassembled species (Fig. 1c,d). Negative-stain electron microscopy (EM) images indicated both nanoparticles to be well-assembled with expected sizes [25,26] (Fig. 1d). Two-dimensional class average revealed more detailed structural features of the nanoparticles, which were consistent with previous published structures of the two nanoparticles. These data indicated the ferritin and LuS nanoparticles were compatible with the SpyTag and glycosylation site addition. These alterations were well tolerated, allowing for robust nanoparticle assembly. To verify glycosylation of LuS- and ferritin-SpyTag nanoparticles, we performed PNGase F digestion and checked for glycan cleavage through SDS-PAGE (Fig. 1e). Both nanoparticles showed a band shift in the presence of PNGase F, indicating the presence of *N*-liked glycan on the nanoparticles and its removal by the amidase digestion. While the glycan cleavage in LuS-N71-SpyTag is distinct, it is less apparent in ferritin-N96-SpyTag, likely due to incomplete glycosylation of

ferritin-N96-SpyTag and multiple bands of ferritin on SDS-PAGE. Ferritin has been observed to exhibit a single band on SDS-PAGE in some studies [2] but multiple bands in others [16,31], presumably due to protease cleavage at the C terminus or incomplete biosynthesis in certain expression systems. However, these different sized ferritin molecules assembled correctly as nanoparticles with expected dimensions as indicated by SEC and EM (Fig. 1c,e).

Conjugation of RSV F-SpyCatcher to LuS-N71-SpyTag displays prefusion RSV F 'DS2'-trimers homogenously on the surface of the LuS-N71-Spylinked-RSV F nanoparticle

With no effective licensed vaccine against respiratory syncytial virus (RSV), the causative agent for a prevalent childhood disease that results in approximately 60,000 hospitalizations and 10,000 annual deaths in the US, developing an immunogen capable of eliciting protection is of paramount importance [32]. Previous efforts in developing a vaccine capable of eliciting protective antibodies have resulted in identification of RSV trimers stabilized in its prefusion conformation, RSV F DS-Cav1 (DS-Cav1) and RSV F DS2 (DS2) [21,33]. DS2 was shown to elicit higher RSV neutralization responses than DS-Cav1 [33]. With this as our motivation and as a test case for our nanoparticle SpyTag:SpyCatcher system, we investigated the feasibility of displaying DS2 in the context of nanoparticle immunogens.

We prepared DS2 coupled to SpyCatcher (hereafter referred to as RSV F-SpyCatcher) by genetic engineering to append SpyCatcher to the C-terminus of RSV F after a 5 residue (GGSGG) linker. After expression and purification, we conjugated the purified RSV F-SpyCatcher to the purified 60-mer LuS-N71-SpyTag nanoparticle (Figure 2a). SEC profiles of the two components revealed that LuS-N71-SpyTag eluted around 13 mL and RSV F-SpyCatcher eluted near 15 mL on Superdex 200 Increase 10/300 column (GE Health Sciences) (Fig.2b). The conjugation mixture was loaded on the SEC column and the conjugated LuS-N71-SpyLinked-RSV F-SpyCatcher

nanoparticle (LuS-N71-SpyLinked-RSV F) eluted in a new peak at ~10 mL (Fig. 2b). SDS-PAGE showed the appearance of species of larger molecular weight of ~90 kDa in the conjugation mixture, followed by bands of residual LuS-N71-SpyTag monomer and RSV F-SpyCatcher components at 20 kDa and 60 kDa, respectively (Fig. 2c), confirming the success of the conjugation reaction. To verify particle integrity after conjugation, we performed negative stain EM following SEC purification. LuS-N71 -SpyTag conjugated with RSV F-SpyCatcher efficiently produced uniform particles with a core diameter of 18.2 ± 1.0 nm decorated with trimer spike of 11.4 ± 0.8 nm in length (Fig. 2d). We then confirmed the prefusion state of the LuS-N71-SpyLinked RSV F nanoparticle through surface plasmon resonance using RSV prefusion F specific antibodies D25 (site Ø) and MPE8 (site III) (Fig. 2e) [21]. Notably, RSV F on nanoparticles showed enhanced on-rate to the apex-targeting D25 and reduced on-rate to the equatorial targeting MPE8 versus trimeric RSV F, a crucial antigenic characteristic signifying appropriate nanoparticle display [3].

Conjugation of RSV prefusion F-SpyCatcher to ferritin-SpyTag produces uniform ferritin-RSV F nanoparticles

Having produced successfully the LuS-N71-SpyLinked-RSV F nanoparticle, we next set out to conjugate the 24-mer ferritin-N96-SpyTag with RSV F-SpyCatcher in the same manner (Fig. 3a). SEC of ferritin-N96-SpyTag nanoparticle showed a peak at around 16-17 mL, slightly slower than RSV F-SpyCatcher (Fig. 3b). Negative stain EM revealed that ferritin-N96-SpyTag formed nanoparticle of the expected size (Fig. 1c). The conjugation mixture of ferritin-N96-SpyTag with RSV F-SpyCatcher exhibited a peak at ~10 mL (void volume of the SEC column), suggesting successful formation of the conjugation product (referred to as ferritin-RSV F) (Fig. 3b). SDS-PAGE demonstrated the appearance of a new band at ~90 kDa, the expected size of

ferritin-N96-SpyLinked-RSV F nanoparticle, with residual ferritin-N96-SpyTag at around 20 kDa (Fig. 3c). To confirm the formation of ferritin-N96-SpyLinked-RSV F nanoparticle, we performed negative stain EM, which showed well-formed nanoparticles with the expected size and shape, displaying trimer spikes around the ferritin nanoparticle (Fig. 3d).

To verify the conserved prefusion state of the conjugated RSV F trimer, we measured the binding of ferritin-N96-SpyLinked-RSV F to D25 and MPE8 IgGs through SPR (Fig. 3e). Importantly, we observed the on-rate to increase for D25, which recognizes an epitope at the trimer apex, but the on-rate to decrease for MPE8, which recognizes an equatorial epitope on the trimer, similar to the observation for LuS-N71-SpyLinked-RSV F.

Displaying PIV3 F glycoprotein trimer on LuS nanoparticle via SpyTag:SpyCatcher conjugation improves antigenicity of the F trimer head region

To demonstrate the plug-and-play versatility of the SpyTag:SpyCatcher nanoparticle system, we produced PIV3 F glycoprotein trimer [34] as a fusion protein with SpyCatcher at the C terminus and conjugated with the LuS-N71-SpyTag nanoparticle (Fig. 4, a-c), similar to that described above for the conjugation of RSV F-SpyCatcher. PIV3 is a prevalent human parainfluenza virus that causes respiratory illnesses, especially in infants and young children [35,36]. The conjugation mixture of PIV3 F-SpyCatcher and LuS-N71-SpyTag was loaded onto the SEC column to purify the conjugated nanoparticle product LuS-N71-SpyLinked-PIV3 F from unconjugated nanoparticles and the PIV3 F SpyCatcher trimer (Fig. 4b). SDS-PAGE analysis revealed that the conjugated product had the expected molecular weight and there was not unconjugated PIV3 F-SpyCatcher in the conjugation mixture, indicating that all LuS subunits of the nanoparticle were conjugated with PIV3 F (Fig. 4c). The PIV3 F conjugated nanoparticle was

further verified through negative stain EM, which showed clearly trimer spikes decorating the LuS nanoparticle with the expected size (Fig. 4d).

Having produced nanoparticles of LuS-N71-SpyTag conjugated with PIV3 F-SpyCatcher, we next evaluated binding of LuS-N71-SpyLinked-PIV3 F with antibodies PIA174 and PIA75 [34], using SPR (Fig. 4e). The head-targeting antibody PIA174 showed an improved binding to LuS-N71-SpyLinked-PIV3 F relative to its binding to PIV3 F-SpyCatcher. The stem-targeting antibody PIA75, however, showed a decreased binding to LuS-N71-SpyLinked-PIV3 F compared with PIV3 F-SpyCatcher.

Conjugation of SARS-CoV-2 spike (S) trimer to LuS nanoparticle via SpyTag:SpyCatcher displays the S trimers homogeneously on the nanoparticle surface

Severe acute respiratory syndrome coronavirus 2 (SARS-CoV-2) caused COVID-19 pandemic that have recently caused severely worldwide disruptions [37]. An effective vaccine against SARS-CoV-2 and related coronaviruses is urgently needed. The SARS-CoV-2 spike (S) glycoprotein trimer is critical for the virus-cell membrane fusion and thus a target for vaccine development [23,24]. To test the versatility of our plug-and-play SpyTag:SpyCatcher nanoparticle system, we expressed and purified CoV-2 S trimers fused with a C-terminal SpyCatcher and conjugated to the LuS-N71-SpyTag nanoparticle (Fig. 5, a-c).

The conjugation mixture was loaded onto an SEC column to purify the conjugated nanoparticle product LuS-N71-SpyLinked-CoV S from unconjugated LuS-N71-SpyTag and CoV-2 S SpyCatcher (Fig. 5b). SDS-PAGE analysis revealed the conjugated product to have the expected molecular weight, and unconjugated SARS-CoV-2 S-SpyCatcher was not observed after conjugation, indicating all LuS subunits to be conjugated with SARS-CoV-2 S (Fig. 5c). Negative stain EM showed LuS-N71-SpyLinked-CoV-2 S nanoparticle to exhibit the expected size with

SARS-CoV-2 S trimers displaying on the LuS nanoparticle surface (Fig. 5d). SPR measurements showed LuS-N71-SpyLinked-SARS-CoV-2 S to bind to CR3022 [38,39], an antibody targeting the receptor-binding domain (RBD), indicating successful nanoparticle presentation of the SARS-CoV-2 S trimer using the LuS-SpyTag:SpyCatcher system.

Discussion

Nanoparticle-based immunogens can induce potent neutralizing antibodies [2,3,40] and thus may be promising vaccine candidates. To develop nanoparticle vaccine immunogens, rapid and efficient methods would be helpful for producing nanoparticle scaffolds that can be mixed and matched with different immunogens. Previous efforts utilizing the spontaneous isopeptide bond formation with the SpyTag:SpyCatcher system for nanoparticle surface display of immunogens [11-16] have proven the versatility of this system for antigen display. However, none of these previousy published reports utilized mammalian expression allowing for post-translational modifications, such as *N*-linked glycosylation. Here, we describe two nanoparticle platforms, lumazine synthase and ferritin, for the display of trimeric viral protein immunogens using the SpyTag:SpyCatcher system. By adding *N*-linked glycosylation sites to nanoparticle monomers, we were able to produce SpyTag-coupled nanoparticles through mammalian cell culture. Conjugation of SpyTag-nanoparticles with SpyCatcher-coupled RSV F, PIV3 F and CoV-2 S trimers resulted in proper particle assembly.

LuS and ferritin nanoparticle platforms vary in the number of molecules displayed on surfaces. LuS-N71-SpyTag contains 60 SpyTags whereas ferritin-N96-SpyTag has 24 displayed on surface, available for SpyCatcher-carrying molecules to couple to. Both platforms showed efficient conjugation of trimeric immunogens and formed nanoparticle rapidly under physiological conditions for RSV F, PIV3 F and CoV-2 S trimers. One advantage of the LuS nanoparticle is the

high efficiency of its particle assembly. The glycosylated LuS-N71-SpyTag assembled into a homogenous particle that exhibited a single peak in size exclusion chromatography.

To demonstrate the versatility of our SpyTag-displaying nanoparticles in immunogen development, we conjugated them to three viral antigens of vaccine interest, the DS2-preF stabilized RSV F [33], a DS2-stabilized version of PIV3 F [34], and the 2P-stabilized version of SARS-CoV-2 S [24]. In each of these, we appended the SpyCatchter after the 'foldon' heterologous trimeric stabilization motif [41]. In all three cases, we observed high conjugation efficiency. It will be interesting to see if our plug and play platform will allow for the incorporation of different molecules on multiple nanoparticles. Such molecules could include not only trimeric viral immunogens, but immunostimulatory components, or molecules targeting antigen presenting cells. Thus the LuS- and ferritin-SpyTag displaying nanoparticles described here, may be amendable to mix-and-match display of immunogens and immunostimulatory or targeting components.

Materials and Methods

Protein production and purification

For protein expression, 3 ml of Turbo293 transfection reagent (Speed BioSystems) was mixed with 50 ml Opti-MEM medium (Life Technology) and incubated at room temperature for 5 min. 1 mg plasmid DNAs was mixed with 50 ml of Opti-MEM medium in a separate tube, and the mixture added to the Turbo293 Opti-MEM mixture. The transfection mixture was incubated for 15 min at room temperature then added to 800 ml of Expi293 cells (Life Technology) at 2.5 million cells/ml. The transfected cells were incubated overnight in a shaker incubator at 9% CO2, 37 °C, and 120 rpm. On the second day, about 100 ml of Expi293 expression medium was added and additional 4 days. On day 5 post transfection, supernatants were harvested, filtered. Proteins were

purified from the supernatant using Ni-NTA and strep chromatography, consecutively, followed by size exclusion column on Superdex 200 Increase 10/300 GL in PBS.

LuS- and ferritin- SpyTag conjugations

A 1:1 molar ratio of LUS- or ferritin-SpyTag and immunogen-SpyCatcher components were combined and incubated at ambient temperature for approximately 3 hours, followed by size exclusion column on Superdex200 Increase 10/300 GL in PBS to separate conjugated products from residual components. The conjugated nanoparticle product was then run through SDS-PAGE to verify conjugation and analyzed by negative-stain EM.

Negative-stain electron microscopy (EM)

Samples were diluted to 0.02-0.05 mg/ml with a buffer containing 10 mM HEPES, pH 7, and 150 mM NaCl. A 4.7-µl drop of the diluted sample was applied to a glow-discharged carbon-coated copper grid for approximately 15 s. The drop was removed using blotting paper, and the grid was washed three times with 4.7-µl drops of the same buffer. Adsorbed proteins were negatively stained by applying consecutively three 4.7-µl drops of 0.75% uranyl formate and removing each drop with filer paper. Micrographs were collected using SerialEM [42] on an FEI Tecnai T20 electron microscope operated at 200 kV and equipped with an Eagle CCD camera or using EPU on a ThermoFisher Talos F200C electron microscope operated at 200 kV and equipped with a Ceta CCD camera. The pixel size was 0.44 and 0.25 nm for Tecnai T20 and Talos F200C, respectively. Particles were picked automatically using in-house written software (Y.T., unpublished). Reference-free 2D classification was performed with Relion 1.4 [43] and SPIDER [44]. The dimensions of VLP cores and spikes were measured with e2display.py program from EMAN2.1 software package [45] using a representative micrograph (LuS-N71-SpyLinked–CoV-2 S) or 2D class average

images (all other VLPs). For CoV-2 nanoparticles we observed increased structural content at low pH, whereas the other micrographs were collected at physiological pH.

Surface Plasmon Resonance (SPR)

To prepare the chips (GE Healthcare Life Sciences CM5 chips), antibody IgG were immobilized onto the chip by amine coupling to ~100-1000 response units (RU) depending the level of binding of each trimer and nanoparticle pair to antibodies. To measure binding of SpyCatcher proteins and and nanoparticles, a dilution series of SpyCatcher-linked proteins and nanoparticles were flowed through the IgG sensor chip for 200 s followed by 800 s of dissociation at a flow rate of 30 μL/min. The starting trimer concentration for each sample was 200 nM. Sensor chip surfaces were regenerated after each injection following manufacture instructions with Glycine 2.5 (GE Healthcare Life Sciences 10 mM glycine -HCl at pH 2.5) at a flow rate of 40 μL/min for 180 s.

Data availability

All relevant data are within the paper and its Supporting Information files.

Acknowledgements

We thank T. Beaumont and H. Spits for antibody D25, A. Lanzavecchia for antibodies PIA174, PIA75 and MPE8, J. Stuckey for assistance with figures, and members of the Vaccine Research Center for discussions or comments on the manuscript. Support for this work was provided by the Intramural Research Program of the Vaccine Research Center, National Institute of Allergy and Infectious Diseases, National Institutes of Health. This project has been funded in part with Federal funds from Frederick National Laboratory for Cancer Research, NIH, under Contract No. HHSN261200800001E (Y. Tsybovsky). The content of this publication does not necessarily

reflect the views or policies of the Department of Health and Human Services, nor does mention of trade names, commercial products, or organizations imply endorsement by the U.S. Government.

Author contributions

B.Z. and C.W.C. designed research with B.Z. heading protein design and production; B.Z., C.W.C, A.S.O., and R.V. produced nanoparticle and trimer proteins; C.W.C. and B.Z. prepared trimer-coupled nanoparticles and performed antigenic assessments; Y.T. performed negative-stain EM; S.W. assisted with manuscript assembly; T.Z. provided design for SARS-CoV 2 S protein; G.S-J. provided the design for PIV3 F protein. B.Z., C.W.C., S.W., and P.D.K. wrote the paper, with all other authors providing revisions and comments. P.D.K. supervised studies.

Competing interests

The author(s) declare no competing interests.

References

1 Lopez-Sagaseta, J., Malito, E., Rappuoli, R. & Bottomley, M. J. Self-assembling protein nanoparticles in the design of vaccines. *Comput Struct Biotechnol J* **14**, 58-68, doi:10.1016/j.csbj.2015.11.001 (2016).

2 Kanekiyo, M. *et al.* Self-assembling influenza nanoparticle vaccines elicit broadly neutralizing H1N1 antibodies. *Nature* **499**, 102-106, doi:10.1038/nature12202 (2013).

3 Marcandalli, J. *et al.* Induction of Potent Neutralizing Antibody Responses by a Designed Protein Nanoparticle Vaccine for Respiratory Syncytial Virus. *Cell* **176**, 1420-1431 e1417, doi:10.1016/j.cell.2019.01.046 (2019).

4 Swanson, K. A. *et al.* A respiratory syncytial virus (RSV) F protein nanoparticle vaccine focuses antibody responses to a conserved neutralization domain. *Sci Immunol* **5**, doi:10.1126/sciimmunol.aba6466 (2020).

5 Cavelti-Weder, C. *et al.* Development of an Interleukin-1beta Vaccine in Patients with Type 2 Diabetes. *Mol Ther* **24**, 1003-1012, doi:10.1038/mt.2015.227 (2016).

6 Cornuz, J. *et al.* A vaccine against nicotine for smoking cessation: a randomized controlled trial. *PLoS One* **3**, e2547, doi:10.1371/journal.pone.0002547 (2008).

7 Zakeri, B. *et al.* Peptide tag forming a rapid covalent bond to a protein, through engineering a bacterial adhesin. *Proc Natl Acad Sci U S A* **109**, E690-697, doi:10.1073/pnas.1115485109 (2012).

8 Marini, A. *et al.* A Universal Plug-and-Display Vaccine Carrier Based on HBsAg VLP to Maximize Effective Antibody Response. *Front Immunol* **10**, 2931, doi:10.3389/fimmu.2019.02931 (2019).
9 He, L. *et al.* Presenting native-like trimeric HIV-1 antigens with self-assembling nanoparticles. *Nat Commun* **7**, 12041, doi:10.1038/ncomms12041 (2016).
10 Yassine, H. M. *et al.* Hemagglutinin-stem nanoparticles generate heterosubtypic influenza protection. *Nat Med* **21**, 1065-1070, doi:10.1038/nm.3927 (2015).
11 Escolano, A. *et al.* Immunization expands B cells specific to HIV-1 V3 glycan in mice and macaques. *Nature* **570**, 468-473, doi:10.1038/s41586-019-1250-z (2019).
12 Govasli, M. L., Diaz, Y. & Puntervoll, P. Virus-like particle-display of the enterotoxigenic Escherichia coli heat-stable toxoid STh-A14T elicits neutralizing antibodies in mice. *Vaccine* **37**, 6405-6414, doi:10.1016/j.vaccine.2019.09.004 (2019).
13 Janitzek, C. M. *et al.* Bacterial superglue generates a full-length circumsporozoite protein virus-like particle vaccine capable of inducing high and durable antibody responses. *Malar J* **15**, 545, doi:10.1186/s12936-016-1574-1 (2016).
14 Thrane, S. *et al.* Bacterial superglue enables easy development of efficient virus-like particle based vaccines. *J Nanobiotechnology* **14**, 30, doi:10.1186/s12951-016-0181-1 (2016).
15 Brune, K. D. *et al.* Plug-and-Display: decoration of Virus-Like Particles via isopeptide bonds for modular immunization. *Sci Rep* **6**, 19234, doi:10.1038/srep19234 (2016).
16 Wang, W. *et al.* Ferritin nanoparticle-based SpyTag/SpyCatcher-enabled click vaccine for tumor immunotherapy. *Nanomedicine* **16**, 69-78, doi:10.1016/j.nano.2018.11.009 (2019).
17 Duan, H. *et al.* Glycan Masking Focuses Immune Responses to the HIV-1 CD4-Binding Site and Enhances Elicitation of VRC01-Class Precursor Antibodies. *Immunity* **49**, 301-311 e305, doi:10.1016/j.immuni.2018.07.005 (2018).
18 Ingale, J. *et al.* Hyperglycosylated stable core immunogens designed to present the CD4 binding site are preferentially recognized by broadly neutralizing antibodies. *J Virol* **88**, 14002-14016, doi:10.1128/JVI.02614-14 (2014).
19 Pantophlet, R., Wilson, I. A. & Burton, D. R. Hyperglycosylated mutants of human immunodeficiency virus (HIV) type 1 monomeric gp120 as novel antigens for HIV vaccine design. *J Virol* **77**, 5889-5901 (2003).
20 Rey, F. A. & Lok, S. M. Common Features of Enveloped Viruses and Implications for Immunogen Design for Next-Generation Vaccines. *Cell* **172**, 1319-1334, doi:10.1016/j.cell.2018.02.054 (2018).
21 McLellan, J. S. *et al.* Structure-based design of a fusion glycoprotein vaccine for respiratory syncytial virus. *Science* **342**, 592-598, doi:10.1126/science.1243283 (2013).
22 Stewart-Jones, G. B. *et al.* Trimeric HIV-1-Env Structures Define Glycan Shields from Clades A, B, and G. *Cell* **165**, 813-826, doi:10.1016/j.cell.2016.04.010 (2016).
23 Walls, A. C. *et al.* Structure, Function, and Antigenicity of the SARS-CoV-2 Spike Glycoprotein. *Cell* **181**, 281-292 e286, doi:10.1016/j.cell.2020.02.058 (2020).
24 Wrapp, D. *et al.* Cryo-EM structure of the 2019-nCoV spike in the prefusion conformation. *Science* **367**, 1260-1263, doi:10.1126/science.abb2507 (2020).
25 Zhang, X., Meining, W., Fischer, M., Bacher, A. & Ladenstein, R. X-ray structure analysis and crystallographic refinement of lumazine synthase from the hyperthermophile Aquifex aeolicus at 1.6 A resolution: determinants of thermostability revealed from structural comparisons. *J Mol Biol* **306**, 1099-1114, doi:10.1006/jmbi.2000.4435 (2001).
26 Cho, K. J. *et al.* The crystal structure of ferritin from Helicobacter pylori reveals unusual conformational changes for iron uptake. *J Mol Biol* **390**, 83-98, doi:10.1016/j.jmb.2009.04.078 (2009).

27 Reddington, S. C. & Howarth, M. Secrets of a covalent interaction for biomaterials and biotechnology: SpyTag and SpyCatcher. *Curr Opin Chem Biol* **29**, 94-99, doi:10.1016/j.cbpa.2015.10.002 (2015).
28 Jardine, J. G. *et al.* HIV-1 broadly neutralizing antibody precursor B cells revealed by germline-targeting immunogen. *Science* **351**, 1458-1463, doi:10.1126/science.aad9195 (2016).
29 Corbett, K. S. *et al.* Design of Nanoparticulate Group 2 Influenza Virus Hemagglutinin Stem Antigens That Activate Unmutated Ancestor B Cell Receptors of Broadly Neutralizing Antibody Lineages. *mBio* **10**, doi:10.1128/mBio.02810-18 (2019).
30 Darricarrere, N. *et al.* Development of a Pan-H1 Influenza Vaccine. *J Virol* **92**, doi:10.1128/JVI.01349-18 (2018).
31 Morris, C. D. *et al.* Differential Antibody Responses to Conserved HIV-1 Neutralizing Epitopes in the Context of Multivalent Scaffolds and Native-Like gp140 Trimers. *mBio* **8**, doi:10.1128/mBio.00036-17 (2017).
32 Graham, B. S. Immunological goals for respiratory syncytial virus vaccine development. *Curr Opin Immunol* **59**, 57-64, doi:10.1016/j.coi.2019.03.005 (2019).
33 Joyce, M. G. *et al.* Iterative structure-based improvement of a fusion-glycoprotein vaccine against RSV. *Nat Struct Mol Biol* **23**, 811-820, doi:10.1038/nsmb.3267 (2016).
34 Stewart-Jones, G. B. E. *et al.* Structure-based design of a quadrivalent fusion glycoprotein vaccine for human parainfluenza virus types 1-4. *Proc Natl Acad Sci U S A* **115**, 12265-12270, doi:10.1073/pnas.1811980115 (2018).
35 Jain, S. *et al.* Community-Acquired Pneumonia Requiring Hospitalization among U.S. Adults. *N Engl J Med* **373**, 415-427, doi:10.1056/NEJMoa1500245 (2015).
36 Jain, S. *et al.* Community-acquired pneumonia requiring hospitalization among U.S. children. *N Engl J Med* **372**, 835-845, doi:10.1056/NEJMoa1405870 (2015).
37 Cucinotta, D. & Vanelli, M. WHO Declares COVID-19 a Pandemic. *Acta Biomed* **91**, 157-160, doi:10.23750/abm.v91i1.9397 (2020).
38 ter Meulen, J. *et al.* Human monoclonal antibody combination against SARS coronavirus: synergy and coverage of escape mutants. *PLoS Med* **3**, e237, doi:10.1371/journal.pmed.0030237 (2006).
39 Yuan, M. *et al.* A highly conserved cryptic epitope in the receptor-binding domains of SARS-CoV-2 and SARS-CoV. *Science*, doi:10.1126/science.abb7269 (2020).
40 Rts, S. C. T. P. Efficacy and safety of RTS,S/AS01 malaria vaccine with or without a booster dose in infants and children in Africa: final results of a phase 3, individually randomised, controlled trial. *Lancet* **386**, 31-45, doi:10.1016/S0140-6736(15)60721-8 (2015).
41 Efimov, V. P. *et al.* Fibritin encoded by bacteriophage T4 gene wac has a parallel triple-stranded alpha-helical coiled-coil structure. *J Mol Biol* **242**, 470-486, doi:10.1006/jmbi.1994.1595 (1994).
42 Mastronarde, D. N. Automated electron microscope tomography using robust prediction of specimen movements. *J Struct Biol* **152**, 36-51, doi:10.1016/j.jsb.2005.07.007 (2005).
43 Scheres, S. H. RELION: implementation of a Bayesian approach to cryo-EM structure determination. *J Struct Biol* **180**, 519-530, doi:10.1016/j.jsb.2012.09.006 (2012).
44 Frank, J. *et al.* SPIDER and WEB: processing and visualization of images in 3D electron microscopy and related fields. *J Struct Biol* **116**, 190-199, doi:10.1006/jsbi.1996.0030 (1996).
45 Tang, G. *et al.* EMAN2: an extensible image processing suite for electron microscopy. *J Struct Biol* **157**, 38-46, doi:10.1016/j.jsb.2006.05.009 (2007).

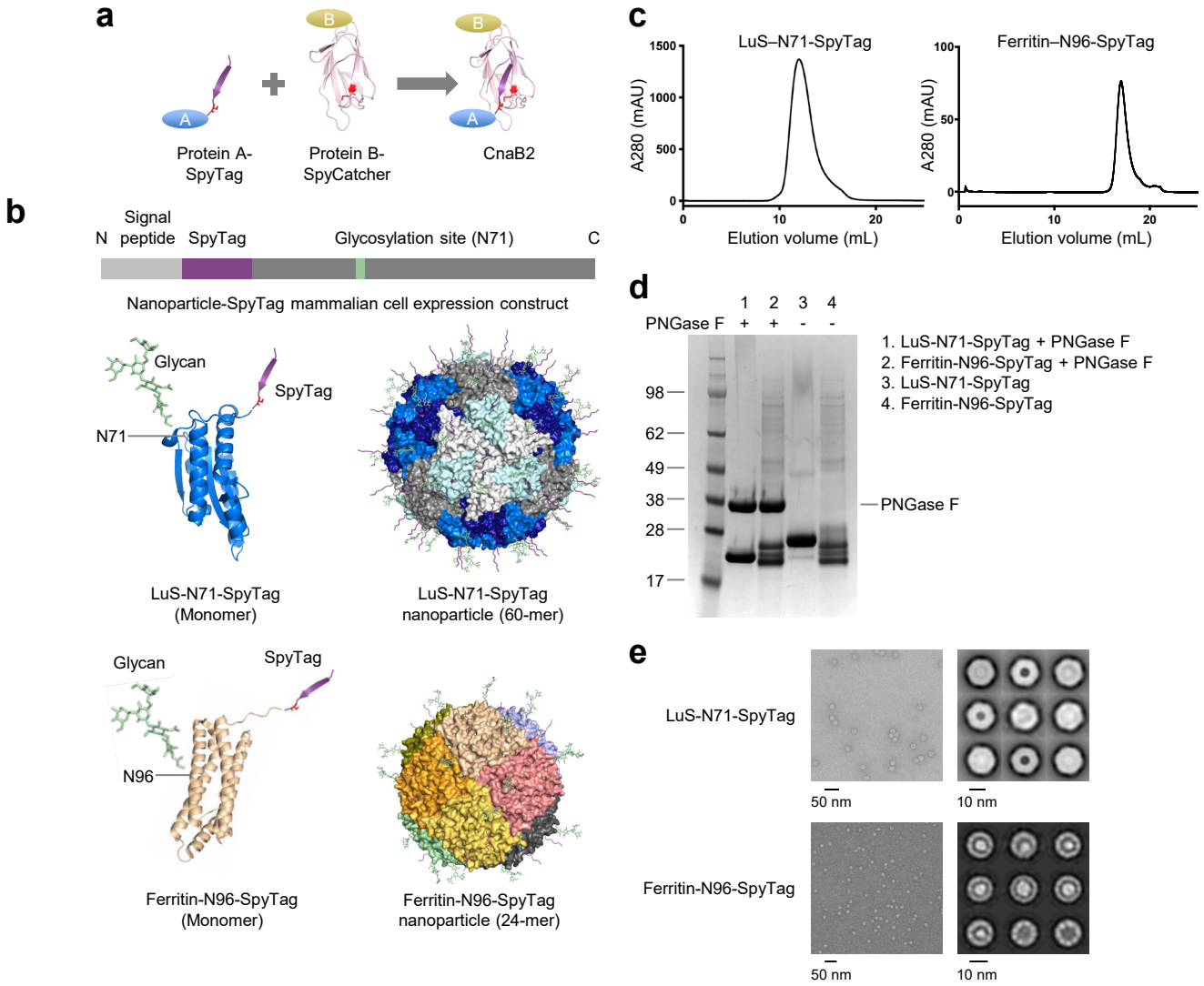

Fig. 1. LuS- and ferritin-nanoparticle scaffolds with N-linked glycan and SpyTag express well as assembled nanoparticles in mammalian cells

(**a**) Schematic diagram showing the separate SpyTag and SpyCatcher to combine through an isopeptide bond as a means to covalently link molecules attached to SpyTag and molecules attached to SpyCatcher. (**b**) Design of expression constructs to produce activated nanoparticles with SpyTag in mammalian cells for conjugating antigens on the nanoparticle surface. Upper panel shows the DNA construct. A SpyTag was placed at the N-terminus of the nanoparticle sequence after the cleavable signal peptide. An N-linked glycosylation site was engineered in the nanoparticle sequence to facilitate protein expression (see Table 1 for more details). Lower panels show the expected structures of the LuS-N71-SpyTag and ferritin-N96-SpyTag monomers and assembled nanoparticles. Both glycan and SpyTag are expected to be on the nanoparticle surface. (**c**) Size exclusion chromatograms confirmed the correct sizes of the nanoparticles. The samples were loaded on a Superdex 200 Increase 10/300 GL column in PBS. Initial run of ferritin-96N-SpyTag nanoparticle revealed tail of small molecular weight species; the chromatogram shown here is the re-run main peak. (**d**) SDS-PAGE of LuS-N71-SpyTag and ferritin-N96-SpyTag in the presence or absence of PNGase F. The position of PNGase F is marked. (**e**) Negative stain EM images (left panels) and 2D class averages (right panels) of LuS-N71-SpyTag and ferritin-N96-SpyTag show the correct assembly of the purified nanoparticles with expected sizes.

Table 1. LuS- and ferritin-nanoparticles with SpyTag require the addition of *N*-linked glycans for expression.

Construct ID	SpyTag	SpyCatcher	Position of glycan	Expression level (mg/L)
Lumazine synthase				
LuS-SpyTag no glycan	x		None	<0.1
LuS-N71-SpyTag*	x		71	**3.0**
LuS-C-SpyCatcher no glycan		x	None	<0.1
LuS-C71-SpyCatcher		x	71	<0.1
LuS-N-SpyCatcher no glycan		x	None	<0.1
LuS-N71-SpyCatcher		x	71	<0.1
Ferritin				
Ferritin-SpyTag no glycan	x		None	<0.1
Ferritin-N96-SpyTag*	x		96	**2.5**
Ferritin-S148-SpyTag*	x		146	**1.0**
Ferritin-SpyCatcher no glycan		x	None	<0.1
Ferritin-N96-SpyCatcher		x	96	<0.1
Ferritin-S148-SpyCatcher		x	146	<0.1

* These constructs showed suitable expression levels.

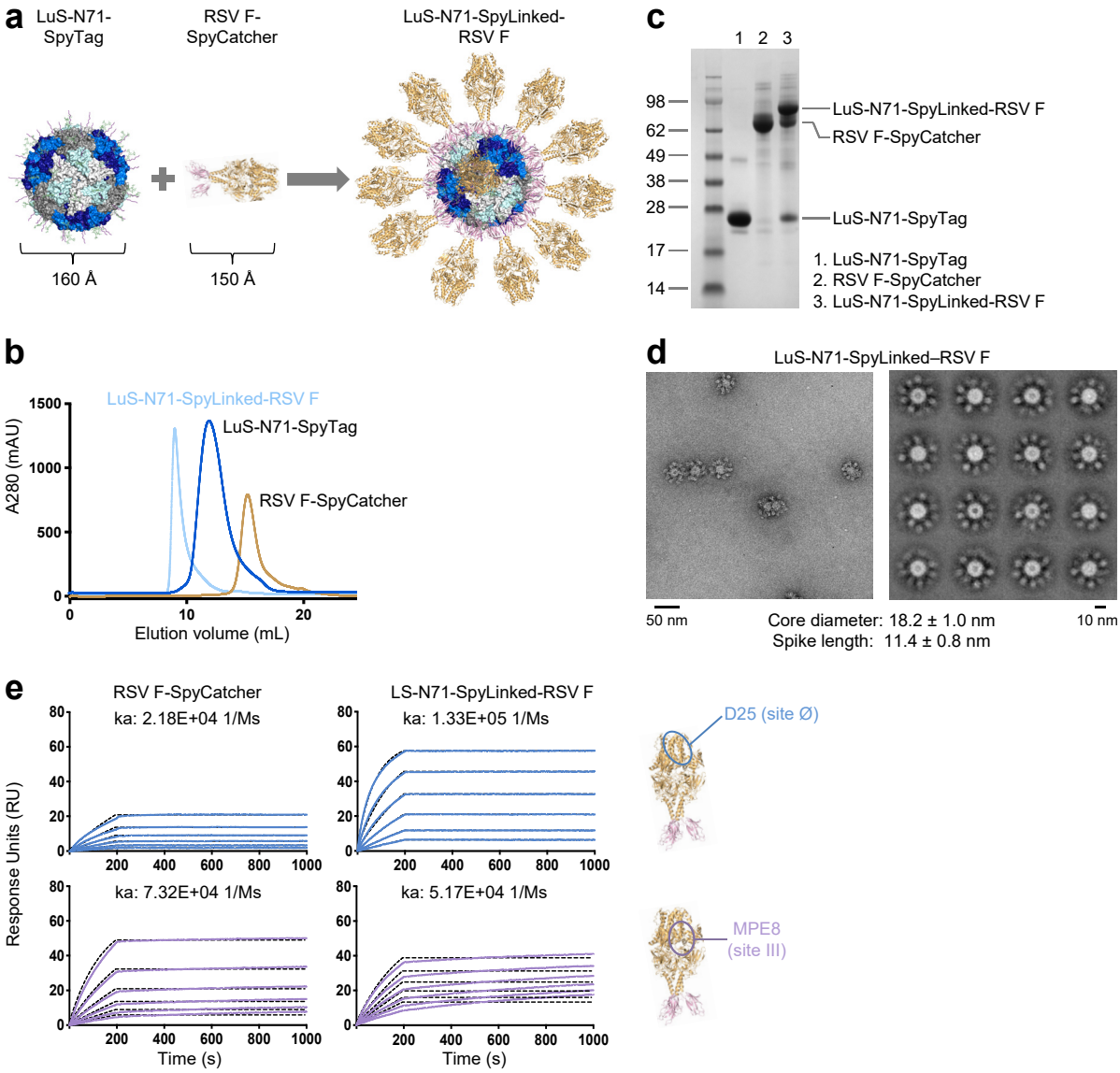

Fig. 2. Conjugation of RSV F-SpyCatcher to LuS-SpyTag displays prefusion RSV F trimer homogenously on the surface of the LuS-N71-SpyLinked-RSV F nanoparticle

(**a**) Schematic diagram showing conjugation of SpyTag-coupled LuS to SpyCatcher-coupled RSV prefusion F trimer to make LuS-N71-SpyLinked-RSV F nanoparticle. (**b**) SEC profiles of LuS-N71-SpyTag, RSV F-SpyCatcher, and the conjugated product LuS-N71-SpyLinked-RSV F on a Superdex 200 Increase 10/300 GL column in PBS. (**c**) SDS-PAGE of LuS-N71-SpyTag (lane 1), RSV F-SpyCatcher (lane 2), and the conjugated LuS-N71-SpyLinked-RSV F nanoparticle product (lane 3), in the presence of DTT. (**d**) Negative stain EM images of the LuS-N71-SpyLinked-RSV F nanoparticle after SEC purification, showing (left panel) a representative micrograph and (right panel) the 2D class averages. (**e**) Surface plasmon resonance of RSV F-SpyCatcher and LuS-N71-SpyLinked-RSV F nanoparticle with prefusion-specific D25 IgG (site Ø) and MPE8 IgG (site III), with IgG coupled to chip and nanoparticle in solution. A concentration series from 200 nM to 1.56 nM of RSV F either as trimer (left) or couped to nanoparticle (right) was measured; k_a values are provided as these have been found to correlate with immunogenicity[3].

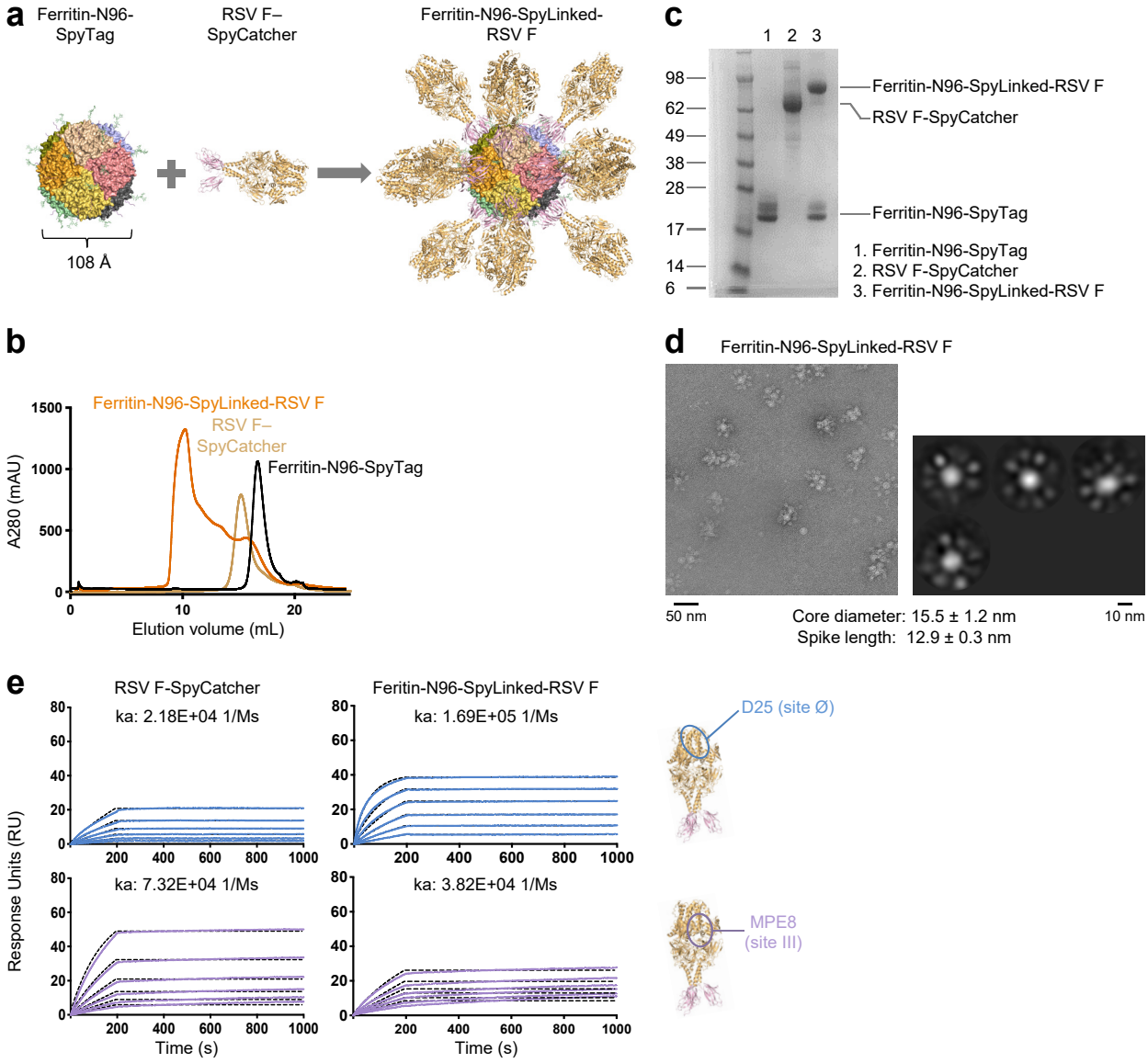

Fig. 3. Conjugation of RSV prefusion F-SpyCatcher to ferritin-SpyTag produces uniform ferritin-RSV F nanoparticles

(**a**) Schematic diagram showing the conjugation process of ferritin-N96-SpyTag and RSV F–SpyCatcher to make ferritin-N96-SpyLinked-RSV F nanoparticle. (**b**) SEC profiles of ferritin-N96-SpyTag, RSV F-SpyCatcher, and the conjugation reaction mixture on a Superdex 200 Increase 10/300 GL column in PBS. (**c**) SDS-PAGE of ferritin-N96-SpyTag (lane 1), RSV F-SpyCatcher (lane 2), and the conjugated ferritin-N96-SpyLinked-RSV prefusion F SpyCatcher nanoparticle product (lane 3), in the presence of DTT. (**d**) Negative stain EM images of the ferritin-RSV F nanoparticle after SEC purification, showing (left panel) a representative micrograph and (right panel) the 2D class averages. (**e**) SPR of RSV F-SpyCatcher and Ferritin-N96-SpyLinked-RSV F nanoparticle with prefusion-specific D25 IgG (site Ø) and MPE8 IgG (site III) using immobilized IgG on sensor chip with nanoparticle and trimer in solution. A concentration series from 200 nM to 1.56 nM of RSV F either as trimer (left) or coupled to nanoparticle (right) was measured; k_a values are provided.

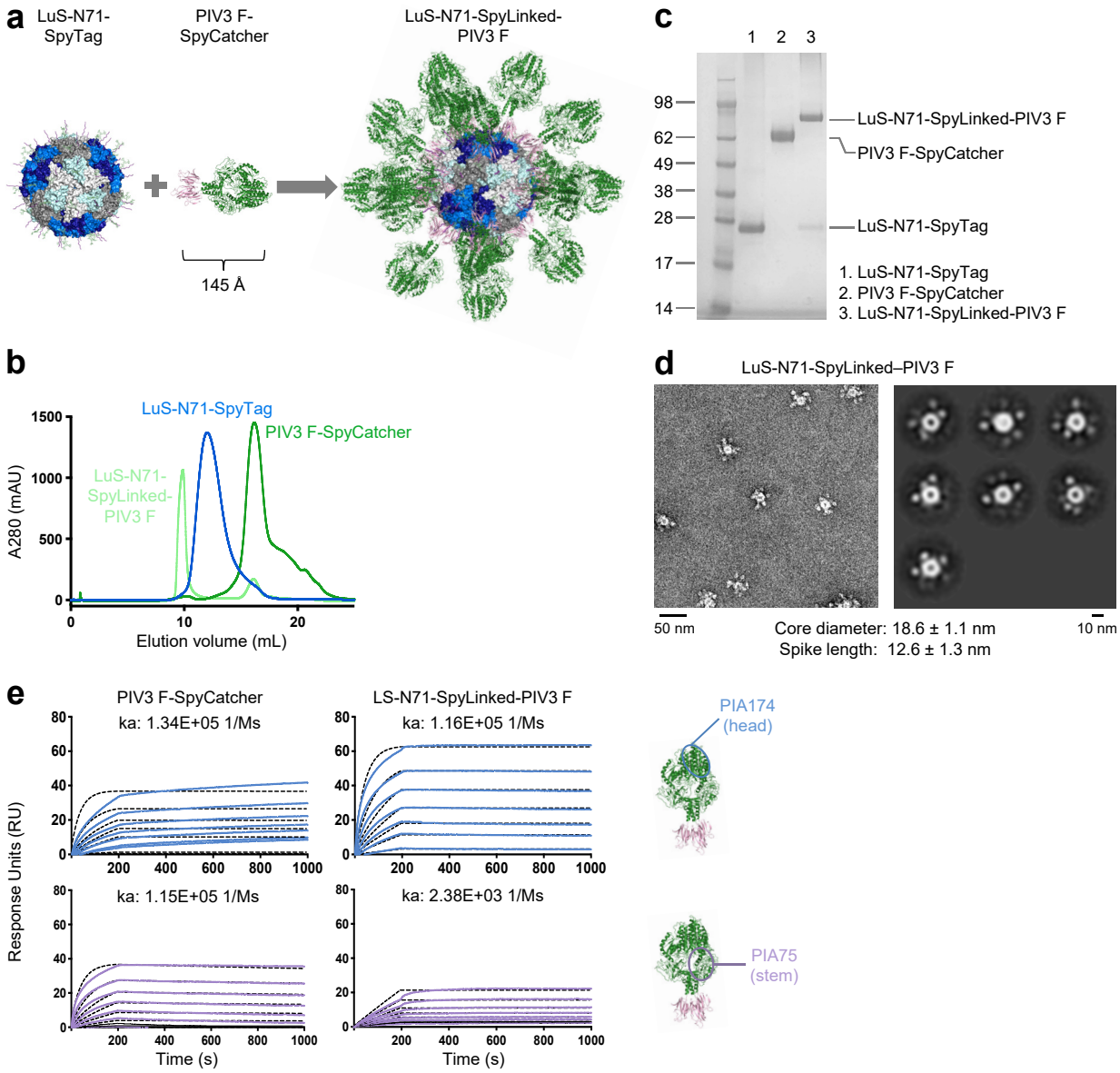

Fig. 4. Conjugation of PIV3 F-SpyCatcher to LuS-SpyTag displays prefusion PIV3 F trimer homogenously on the surface of the LuS-N71-SpyLinked-PIV3 F nanoparticle

(**a**) Schematic of the conjugation between LuS-N71-SpyTag and PIV3 F-SpyCatchert to produce LuS-N71-SpyLinked-PIV3 F nanoparticle (**b**) SEC profiles of PIV3 F-SpyCatcher, LuS-SpyTag, and the conjugated product LuS-N71-SpyLinked-PIV3 F on a Superdex 200 Increase 10/300 GL in PBS. (**c**) SDS-PAGE of LuS-N71 (lane 1), PIV3 F-SpyCatcher (lane 2), and LuS-N71-SpyLinked-PIV3 F conjugation mixture (lanes 3) in the presence of DTT. (**d**) Negative stain EM of LuS-N71-SpyLinked-PIV3 following SEC showing a representative micrograph (left panel) and 2D class averages (right panel). (**e**) SPR measurements of PIV3 F-SpyCatcher and LuS-N71-SpyLinked-PIV3 F were performed using IgG coupled chips with nanoparticle and timer in solution. A concentration series from 200 nM to 1.56 nM of PIV3 F either as trimer (left) or coupled to nanoparticle (right) was measured; k_a values are provided.

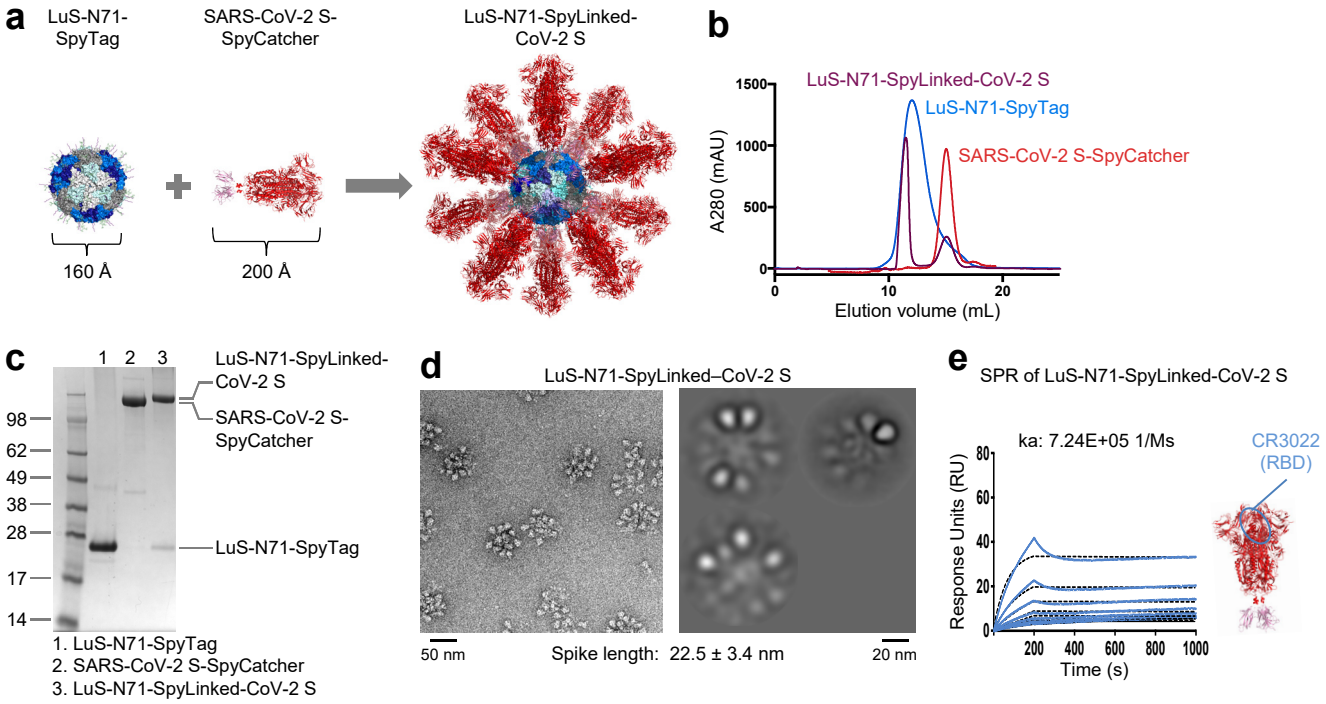

Fig. 5. Conjugation of SARS-CoV-2 S trimer to LuS-SpyTag displays SARS-CoV-2 S trimer on the surface of the LuS-N71-SpyLinked-CoV-2 S nanoparticle

(**a**) Schematic diagram showing conjugation of SpyTag-coupled LuS to SpyCatcher-coupled SARS-CoV-2 spike trimer to make LuS-N71-SpyLinked-CoV-2 S nanoparticle. (**b**) SEC profiles of LuS-N71-SpyTag, SARS-CoV-2 S-SpyCatcher, and the conjugated product LuS-N71-SpyLinked-CoV-2 S on a Superdex 200 Increase 10/300 GL column in PBS. (**c**) SDS-PAGE of LuS-N71-SpyTag (lane 1), SARS-CoV-2 S-SpyCatcher (lane 2), and the conjugation mixture of LuS-N71-SpyTag with SARS-CoV-2 S-SpyCatcher (lane 3) in the presence of DTT. The conjugation mixture (lane 3) shows the conjugated LuS-N71-SpyLinked-CoV-2 S nanoparticle with minor excess of LuS-N71-SpyTag. (**d**) Negative stain EM of the LuS-N71-SpyLinked-CoV-2 S nanoparticle after SEC purification showing representative micrographs (left panel) and 2D class average (right panel). (**e**) SPR response curves for LuS-N71-SpyLinked-CoV-2 S nanoparticle binding with RBD-targeting antibody CR3022 IgG, with IgG coupled to chip and nanoparticle in solution. Because SARS-CoV-2 S-SpyCatcher showed non-specific binding only the coupled nanoparticle is shown. A series of nanoparticle concentrations was analyzed in which the concentration of SARS CoV-2 S coupled to the nanoparticle ranged from 200 nM to 1.56 nM. Observed k_a value provided.